Indian J Phys (August 2025) 99(9):3409–3421
https://doi.org/10.1007/s12648-024-03541-5

ORIGINAL PAPER

Dynamical analysis of multi-soliton and interaction of solitons solutions of nonlinear model arise in energy particles of physics

M M Roshid[1]*, M Rahman[2], M A N Sheikh[3], M Uddin[4], M S Khatun[3] and H -Or- Roshid[3]

[1]Department of Mathematics, Hamdard University Bangladesh, Hamdard Nagar, Gazaria, Munshiganj 1510, Bangladesh

[2]Department of Physics, Uttara University, Turag, Dhaka 1230, Bangladesh

[3]Department of Mathematics, Sunamgonj Science and Technology University, Shantiganj, Sunamganj 3000, Bangladesh

[4]Institute Natural Sciences, United International University, Badda, Dhaka 1212, Bangladesh

Received: 12 September 2024 / Accepted: 31 December 2024 / Published online: 25 January 2025

Abstract: This study explores multi-soliton solutions and their interactions within the framework of the Klein-Fock-Gordon (K-F-G) equation. The K-F-G equation plays a crucial role in modeling relativistic wave phenomena and has diverse applications in describing energy particles in physics. The newly modified simple equation (NMSE) method is employed to analyze multi-soliton solutions and their interactions. Under specific conditions, novel families of solutions are derived and expressed through exponential and hyperbolic functions, as well as their combinations. The NMSE method is particularly effective in generating and analyzing a variety of soliton interactions, including multi-kink and anti-kink solutions, multi-bell-shaped solutions for bright-dark and dark-bright solitons, and combinations of kink, bell-shaped, and periodic solutions. These interactions are further illustrated through 3D visualizations, density plots, and contour maps. The simulation results demonstrate that the NMSE method works efficiently, is simple to use, and has versatility for a wide range of nonlinear evolution equations in computational physics and other interdisciplinary domains.

Keywords: New modified simple equation scheme; Klein-Fock-Gordon equation; Energy particles in physics; Climate action

1. Introduction

Nonlinear evolution equations are essential for modeling complex phenomena across multiple scientific disciplines and engineering fields. They provide a mathematical framework for understanding the temporal evolution of physical quantities or fields in systems where nonlinearity is a key characteristic. These equations are indispensable for understanding and modeling complex phenomena across various domains, and they are applied in several critical areas. In fluid mechanics, the Navier–Stokes equations describe the behavior of fluids. Nonlinear variants of these equations are used to model turbulence, chaotic flows, and vortices in both liquids and gases. These models are vital in understanding weather patterns, ocean currents, and aerodynamics. The nonlinear evolution equations are very important in quantum field theory. They define the nonlinear Schrödinger mode, which shows how wave packets and solitons move in some quantum systems, like Bose–Einstein condensates. In optics, nonlinear evolution equations describe the behavior of light in nonlinear media. They are used to understand phenomena like self-focusing, second-harmonic generation, and the formation of optical solitons, which have applications in telecommunications and laser technology. In population dynamics, nonlinear models are employed in ecology and epidemiology to study population growth, predator–prey interactions, and disease-spreading ways. The Lotka-Volterra equations, for instance, describe the dynamics of interacting species in ecosystems. It is too difficult to execute the exact solution of such nonlinear models. With the progress of soliton theory, different authentic methods to investigate soliton solutions have been proposed and developed, namely, generalized exponential rational function [1], iterative [2], EMAE mapping [3], Simplified Hirota’s [4], Sine–Gordon expansion [5], Modified Kudryashov [6],

*Corresponding author, E-mail: mamunmath307@gmail.com

enhanced modified simple equation [7], a direct [8], $\left(\frac{\varphi'}{\varphi}, \frac{1}{\varphi}\right)$-expansion and GPRE [9], modified simple equation [10–12], New MSE [13], Lie group theoretic [14], simple equation [15], Darboux [16], Crank–Nicholson [17, 18] methods, and so on [19–22].

The study of interaction solutions and multi-soliton solutions for nonlinear evolution equations has become a research hotspot because they can be more applicable to many complex situations in various physical settings than single-wave solutions. A lot of interesting work has been done in the past few years on multi-wave interaction solutions in rich forms for nonlinear evolution equations with constant coefficients [23–28]. Many of the aforementioned techniques [1–18] are capable of providing only traveling wave solutions, not multi-soliton solutions for nonlinear models. However, there are a few methods, such as the multiple exp-function scheme [29, 30], Hirota bilinear method [31–35], Wronskian approach [36, 37], and the New MSE method [38], that can derive various pattern of multi-wave solitons. However, the Wronskian and Hirota bilinear methods are relatively old and may not be suitable for all nonlinear models that cannot be converted into a bilinear form. This is particularly true for non-integrable non-linear models, which are incapable of converting into a bilinear form. The NMSE method can find the multi-wave soliton and how they interact for a non-linear model that can't be integrated. The new MSE method gives direct multi-soliton solutions and shows how they interact with non-linear models, so they don't need to be changed into bilinear forms.

This work executes the multi-soliton solution, the interaction of solitons from the K-F-G equation. For multi-soliton solutions and the interaction of solitons, we use a new modified simple equation scheme [38] for the K-F-G equation. We start the K-F-G equation in the following form:

$$\tau_{tt} + \mu_1\tau_{xx} + \mu_2\tau + \mu_3\tau^3 = 0, \tag{1}$$

where μ_1, μ_2 and μ_3 are arbitrary constants. There are many techniques applied to exact solution from the K-F-G equation such as modified $\left(\frac{G'}{G}\right)$-expansion method and the generalized Kudryashov method [39], ESE scheme, and modified F-expansion approach [40], modified Kudryashov's and extended Kudryashov's methods [41], Sardar sub-equation method [42], and Bifurcation theory [43]. The

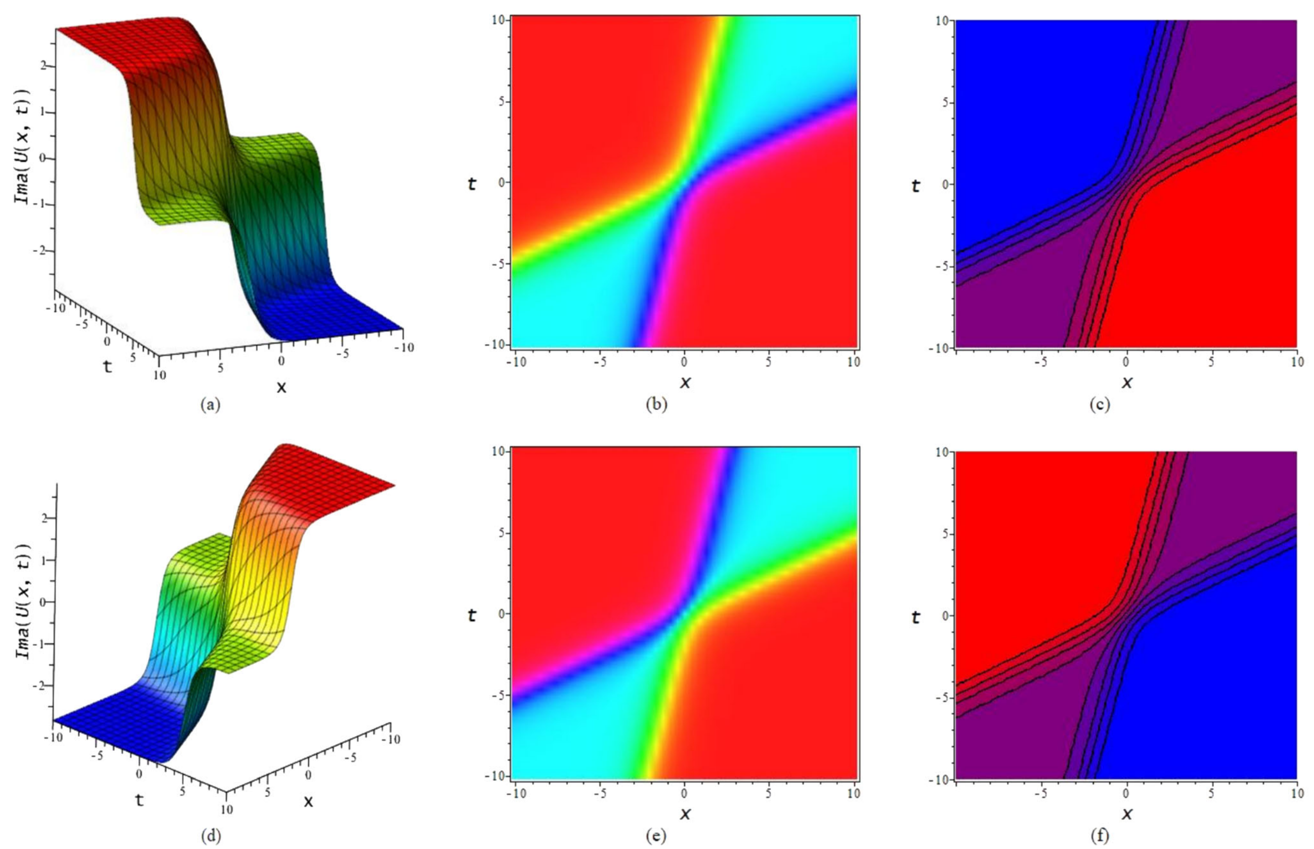

Fig. 1 Feature of the multi-soliton solution of Eq. (17) for the parameters $k_1 = 2,\ k_2 = \omega_1 = 0.5, \omega_2 = 1, \mu_1 = 1, \mu_2 = -2, \mu_3 = -1, l_1 = l_2 = l_3 = l_4 = l_5 = l_6 = 1$. (**a**) and (**d**) are 3-D plots of multi-kink and multi-anti-kink respectively; (**b**) and (**e**) are corresponding density plots; (**c**) and (**f**) are corresponding contour plots

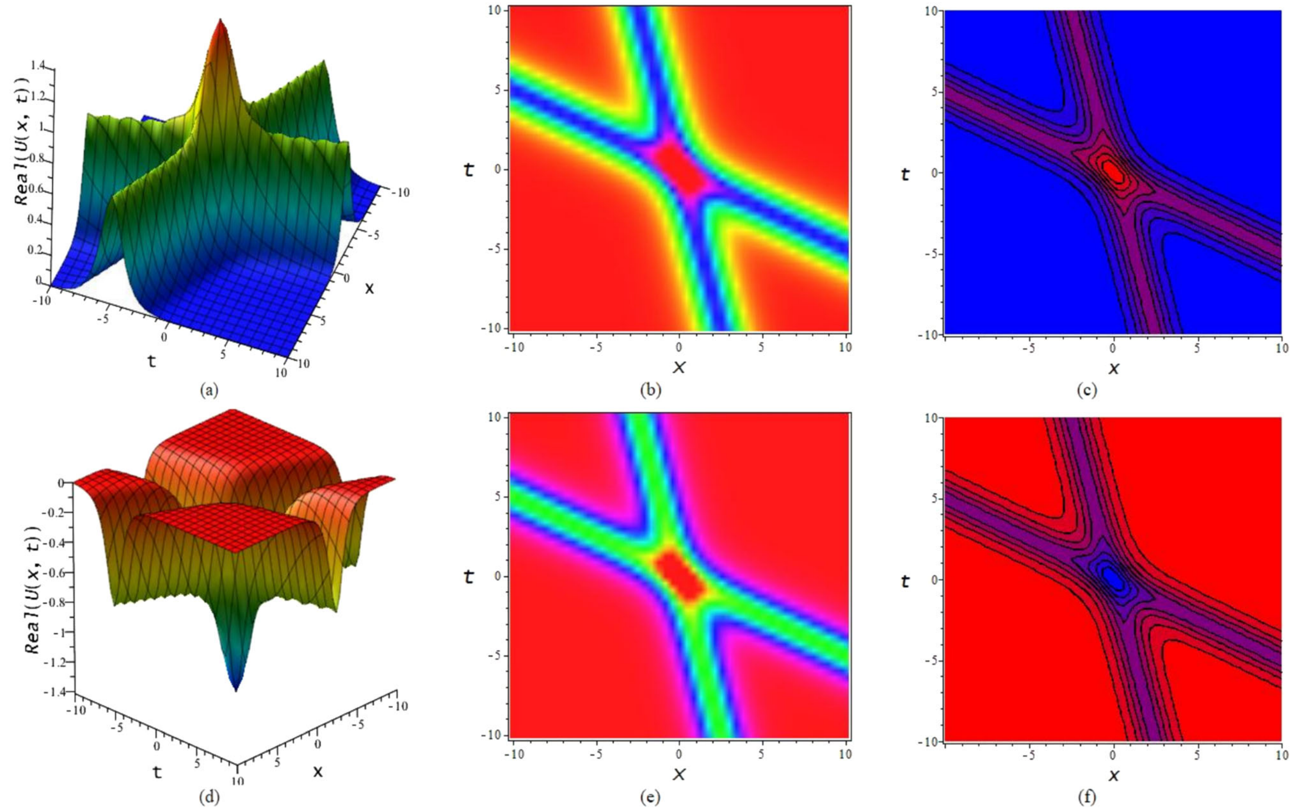

Fig. 2 Feature of the multi-soliton with interaction solution of Eq. (17) for the parameters $k_1 = 2,\ k_2 = 0.5, \omega_1 = -1, \omega_2 = -0.5, \mu_1 = 1, \mu_2 = -2, \mu_3 = -1, l_1 = l_2 = l_3 = l_4 = l_5 = l_6 = 1$. (**a**) and (**d**) are 3-D plots of bright and dark bell-type multi-soliton with their interaction respectively; (**b**) and (**e**) are corresponding density plots; (**c**) and (**f**) are corresponding contour plots

main goal of this work is to integrate multi-soliton solutions and diverse interaction solitons analytically and graphically. There are no methods applied for this model to integrate the multi-soliton and interaction of solitons solution. For the first time, we find the multi-soliton and their interactions for this model. For different parametric values, we show some novel multi-soliton waves and interaction waves with 3D, contour, and density plots, including the multi-kink wave, the multi-anti-kink wave, the interaction of the anti-kink and dark bell wave, the anti-kink and bright bell wave, the two bright bell waves, the two dark bell waves, the bright and dark bell waves, the periodic and singular wave, the interaction solution between the soliton and kink wave, the anti-kink and periodic wave, the kink and periodic wave, the breather wave, and the interaction of the double bright and dark bell wave. We also discussed the behavior of the parameters in the obtained solutions.

This remaining work is systematized as:

- Section 2 discusses the working processes NMSE technique to resolve NLEEs.
- Section 3 describes the multi-soliton solutions, and their interaction for the Klein-Fock-Gordon equation analytically.
- Section 4 illustrates some novel multi-soliton waves and different types of interaction solutions.
- Section 5 delivers an overview of this work.

2. New formation of modified simple equation scheme

In this section, we write the working steps of new formations of the MSE (NMSE) method to solve NLEEs. For this purpose, we study a nonlinear model in the succeeding arrangement:

$$R[\tau] = R(\tau_{tt}, \tau\tau_x, \tau_{xx}, \tau^n \ldots\ldots\ldots), \tag{2}$$

where $\tau = \tau(x, t)$ and R is a function of g.

The technique of the NMSE scheme can be expressed in the succeeding steps:

Step-1: The trial solution of Eq. (2) is:

$$\tau = \sum_{r=0}^{\beta} \sum_{i+j=r}^{\beta} a_i a_{\beta+j} \left(\frac{\varphi_1'(\xi_1)}{\varphi_1'(\xi_1)}\right)^i \left(\frac{\varphi_2''(\xi_2)}{\varphi_1'(\xi_2)}\right)^j, \tag{3}$$

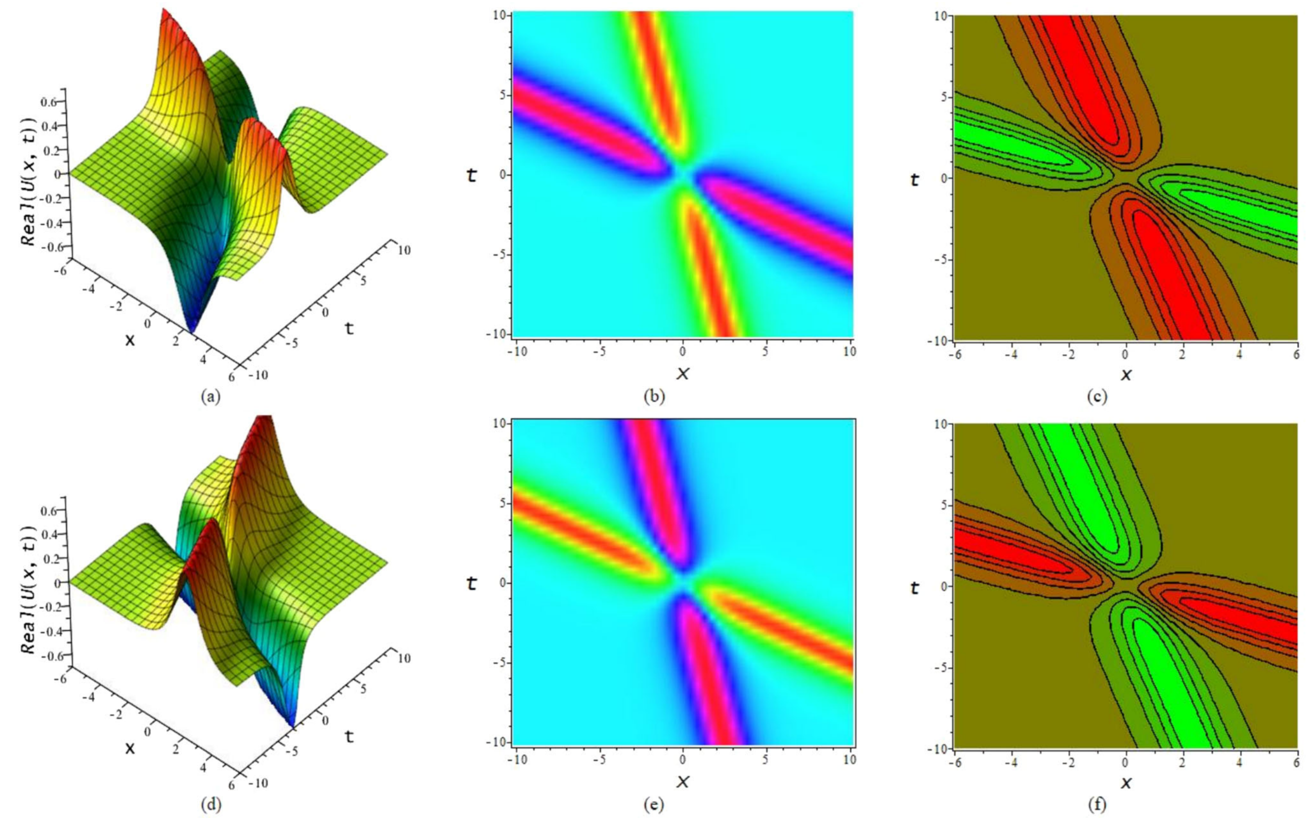

Fig. 3 Feature of the interaction solution of Eq. (17) for the parameters $k_1 = 2,\ k_2 = -\omega_1 = 0.5, \omega_2 = -1, \mu_1 = 1, \mu_2 = -2, \mu_3 = -1, l_1 = l_2 = l_3 = l_4 = l_5 = l_6 = 1$. (**a**) and (**d**) are 3-D plots of interaction with bright and dark bell waves, respectively; (**b**) and (**e**) are corresponding density plots; (**c**) and (**f**) are corresponding contour plots

where $\xi_j = k_j x - \omega_j t; \mathrm{j} = 1, 2$ and $\mathrm{a_i},\ \mathrm{a}_{\beta+\mathrm{j}}$ where $\mathrm{i}, \mathrm{j} = 0, 1, 2, \ldots$ are unknown constants but $\mathrm{a}_\beta \neq 0$.

Step-2: To find the trial solution, we need to find the balance value β which appears from the highest nonlinear and derivative terms in Eq. (2).

Step-3: If we use the trail solution Eq. (3) to Eq. (2), then a polynomial of $\varphi_1^{-\mathrm{i}}, \varphi_2^{-\mathrm{j}}$, and $\varphi_1^{-\mathrm{i}}\varphi_2^{-\mathrm{j}}$ are obtained.

Step-4: To obtain a system of solution, the coefficients of $\varphi_1^{-\mathrm{i}}, \varphi_2^{-\mathrm{j}}$, and $\varphi_1^{-\mathrm{i}}\varphi_2^{-\mathrm{j}}$ are considered to be zero. Then we solved them to estimate the values $\mathrm{a_i}, \mathrm{a_j}, \varphi_1$, and φ_2. After inserting the obtained values in the trial solution, we get the required solutions.

3. Evaluate multi-soliton and interact soliton solution with NMSE scheme

In this section, we implement the NMSE technique to the K-F-G equation. The balance number between τ_{xx} and τ^3 is $\beta = 1$. So, the trial solution of Eq. (1) is

$$u = \mathrm{a}_0 + \mathrm{a}_1\left(\frac{\varphi_1'(\xi_1)}{\varphi_1'(\xi_1)}\right) + \mathrm{a}_2\left(\frac{\varphi_2'(\xi_2)}{\varphi_2'(\xi_2)}\right), \tag{4}$$

where $\xi_r = k_r x - \omega_r t; r = 1, 2$ with $k_r; r = 1, 2$ are the angular speeds and $\omega_r; r = 1, 2$ are wave frequencies. According to this scheme, we get a system of equations.

$$\mu_2 \mathrm{a}_0^3 + \mu_3 \mathrm{a}_0 = 0, \tag{5}$$

$$\mathrm{a}_1\left(\omega_1^2 + \mu_1 \mathrm{k}_1^2\right)\varphi_1''' + \left(3\mu_3 \mathrm{a}_0^2 + \mu_2\right)\varphi_1' = 0, \tag{6}$$

$$\mathrm{a}_2\left(\omega_2^2 + \mu_1 k_2^2\right)\varphi_2''' + + \left(3\mu_3 \mathrm{a}_0^2 + \mu_2\right)\varphi_2' = 0, \tag{7}$$

$$3\mathrm{a}_1\left(-\mu_1 k_1^2 - \omega_1^2\right)\varphi_1''\varphi\varphi_1' + 3\mu_3 a_0 a_1^2 \varphi_1'\varphi_1' = 0, \tag{8}$$

$$3\mathrm{a}_2\left(-\mu_1 k_2^2 - \omega_2^2\right)\varphi_2''\varphi_2' + 3\mu_3 \mathrm{a}_0 \mathrm{a}_2^2 \varphi_2'\varphi_2' = 0, \tag{9}$$

$$\mu_3 \mathrm{a}_1^3 + 2\mu_1 \mathrm{a}_1 k_1^2 + 2\mathrm{a}_1\omega_1^2 = 0, \tag{10}$$

$$\mu_3 \mathrm{a}_2^3 + 2\mu_1 \mathrm{a}_2 k_2^2 + 2\mathrm{a}_2\omega_2^2 = 0, \tag{11}$$

$$3\mu_3 \mathrm{a}_2 \mathrm{a}_1^2 \varphi_1'\varphi_1'\varphi_2' = 0, \tag{12}$$

$$3\mu_3 \mathrm{a}_1 \mathrm{a}_2^2 \varphi_2'\varphi_2'\varphi_1' = 0, \tag{13}$$

$$6\mu_3 \mathrm{a}_1 \mathrm{a}_0 \mathrm{a}_2 \varphi_1'\varphi_2' = 0. \tag{14}$$

Solve the Eq. (5) and Eq. (10) to Eq. (14), we get

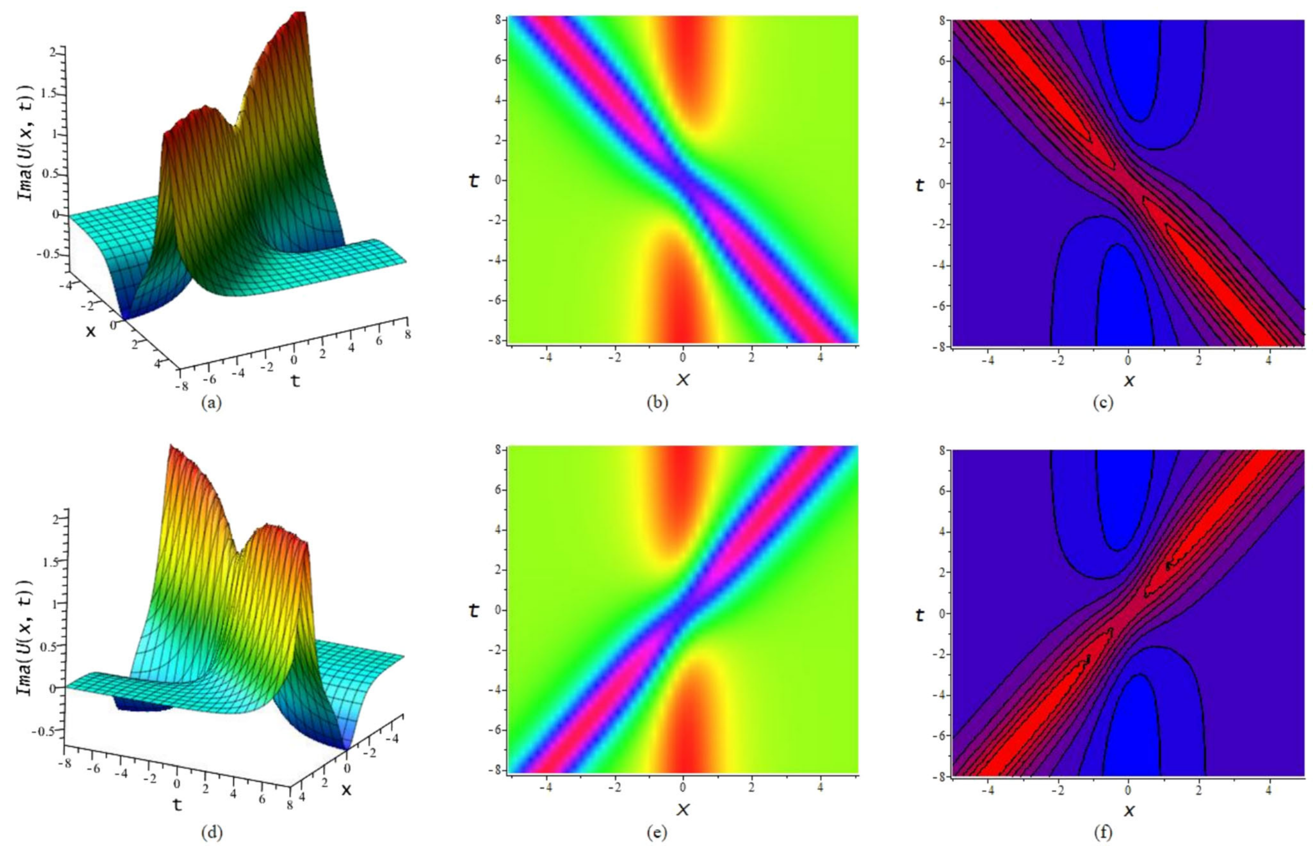

Fig. 4 Feature of the interaction solution of Eq. (17) for the parameters $k_1 = 15,\ k_2 = 1, \omega_1 = 0.01, \omega_2 = 0.5, \mu_1 = 1, \mu_2 = -2, \mu_3 = 1, l_1 = -l_2 = l_3 = l_4 = l_5 = -3l_6 = 1$. (**a**) and (**d**) are 3-D plots of interaction with bright and dark bell waves, respectively; (**b**) and (**e**) are corresponding density plots; (**c**) and (**f**) are corresponding contour plots

$$a_0 = 0, \pm\sqrt{-\frac{\mu_2}{\mu_3}}, a_1 = \sqrt{\frac{2(\mu_1 k_1^2 + \omega_1^2)}{-\mu_3}}, -\sqrt{\frac{2(\mu_1 k_1^2 + \omega_1^2)}{-\mu_3}}, a_2 = \sqrt{\frac{2\left(\mu_1 k_2^2 + \omega_2^2\right)}{-\mu_3}}, -\sqrt{\frac{2\left(\mu_1 k_2^2 + \omega_2^2\right)}{-\mu_3}}$$

Case-01: If $a_0 = 0$ then Eq. (8) and Eq. (9) develop as

$$\varphi_1'' = 0,$$

$$\varphi_2'' = 0.$$

Now the Eq. (6) and Eq. (7) can be written as

$$\varphi_1 = b_0 + b_1\sin(p\xi_1) + b_2\cos(p\xi_1), \tag{15}$$

$$\varphi_2 = b_3 + b_4\sin(q\xi_2) + b_5\cos(q\xi_2). \tag{16}$$

Inset the Eq. (15) and Eq. (16) in Eq. (4), then we attain as

$$u = pa_1\frac{b_1\cos(p\xi_1) - b_2\sin(p\xi_1)}{b_0 + b_1\sin(p\xi_1) + b_2\cos(p\xi_1)} + qa_2\frac{b_4\cos(q\xi_2) - b_5\sin(q\xi_2)}{b_3 + b_4\sin(q\xi_2) + b_5\cos(q\xi_2)}, \tag{17}$$

where $p = \sqrt{\frac{\mu_2}{\mu_1 k_1^2 + \omega_1^2}}, q = \sqrt{\frac{\mu_2}{\mu_1 k_2^2 + \omega_2^2}}, a_1 = \pm\sqrt{\frac{2(\mu_1 k_1^2 + \omega_1^2)}{\mu_3}}, a_2 = \pm\sqrt{\frac{2\left(\mu_1 k_2^2 + \omega_2^2\right)}{\mu_3}},$
$\xi_1 = k_1 x - \omega_1 t$, and $\xi_2 = k_2 x - \omega_2 t$.

Case-02: If $\alpha_0 = \pm\sqrt{-\frac{\mu_2}{\mu_3}}$ then the Eq. (8) and Eq. (9) develop as

$$\varphi_1' = -\sqrt{\frac{(\mu_1 k_1^2 + \omega_1^2)}{2\mu_3}}\varphi_1'', \tag{18}$$

$$\varphi_2' = -\sqrt{\frac{(\mu_1 k_2^2 + \omega_2^2)}{2\mu_2}}\varphi_2''. \tag{19}$$

Injecting Eq. (18) in Eq. (6) and Eq. (19) in Eq. (7), then we accomplish as

$$\varphi_1'' = b_7 e^{r\xi_1}, \tag{20}$$

$$\varphi_2'' = b_9 e^{l\xi_2}, \tag{21}$$

where $b_7,\ b_9$ are free parameters.

From Eq. (18) and Eq. (19) with Eq. (20) and Eq. (21), respectively, we get as

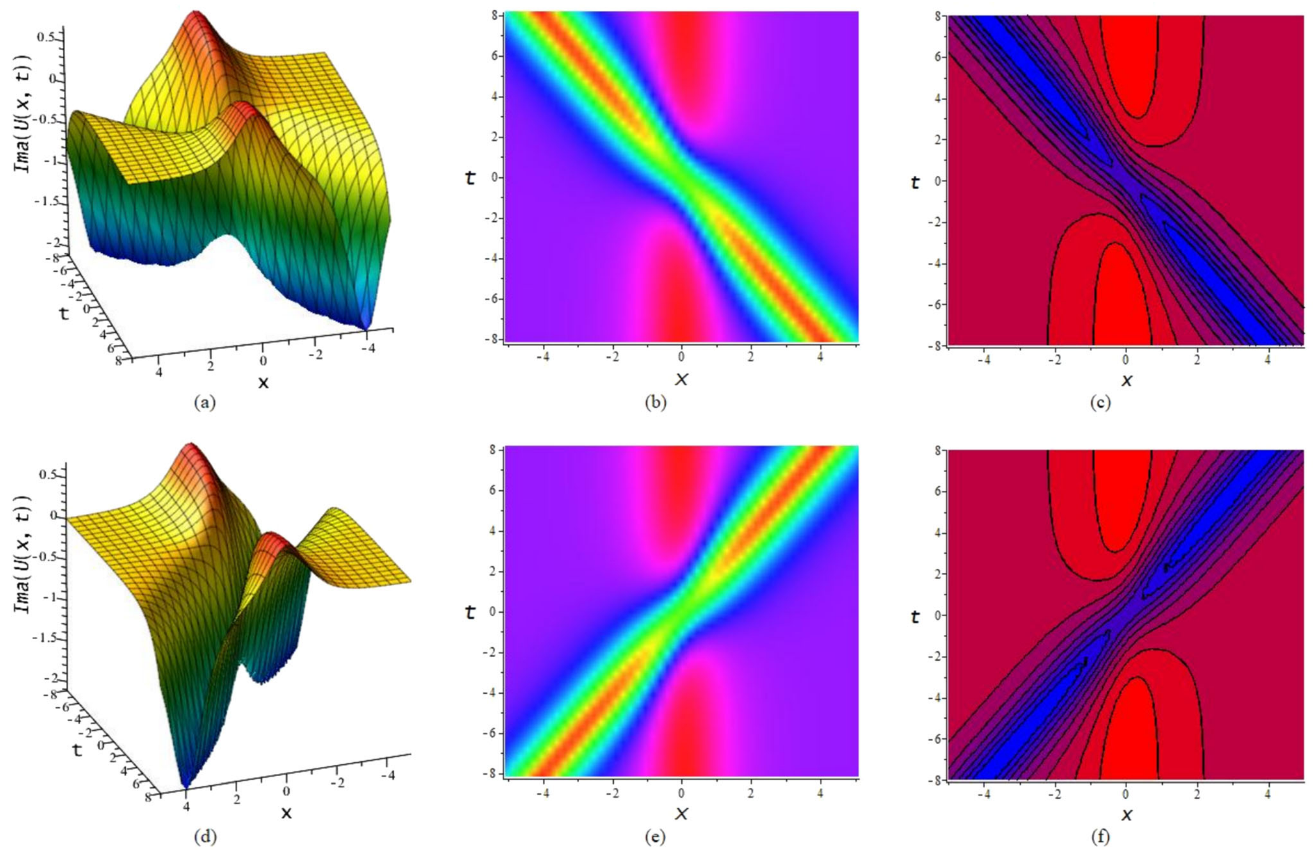

Fig. 5 Feature of the interaction solution of Eq. (17) for the parameters $k_1 = 15,\ k_2 = 1, \omega_1 = 0.01, \omega_2 = 0.5, \mu_1 = 1, \mu_2 = -2, \mu_3 = 1, l_1 = -l_2 = l_3 = l_4 = l_5 = -3l_6 = 1$. (**a**) and (**d**) are 3-D plots of the interaction of double bright and dark bell waves, respectively; (**b**) and (**e**) are corresponding density plots; (**c**) and (**f**) are corresponding contour plots

$$\varphi_1 = b_8 - \frac{(\mu_1 k_1^2 + \omega_1^2)}{2\mu_3} b_7 e^{r\xi_1}, \tag{22}$$

$$\varphi_2 = b_{10} - \frac{(\mu_1 k_2^2 + \omega_2^2)}{2\mu_2} b_9 e^{l\xi_2}, \tag{23}$$

where $b_7, b_8,\ b_9,\ b_{10}$ are free parameters.

The solution of Eq. (4) is

$$u = -\sqrt{-\frac{\mu_2}{\mu_3}} - a_1 \frac{\sqrt{\frac{(\mu_1 k_1^2+\omega_1^2)}{2\mu_2}} b_7 e^{r\xi_1}}{b_8 + \frac{(\mu_1 k_1^2+\omega_1^2)}{2\mu_2} b_7 e^{r\xi_1}} - a_2 \frac{\sqrt{\frac{(\mu_1 k_2^2+\omega_2^2)}{2\mu_2}} b_9 e^{l\xi_2}}{b_{10} + \frac{(\mu_1 k_2^2+\omega_2^2)}{2\mu_2} b_9 e^{l\xi_2}}, \tag{24}$$

where $r = -\sqrt{\frac{2\mu_2}{(\mu_1 k_1^2+\omega_1^2)}}, l = -\sqrt{\frac{2\mu_2}{(\mu_1 k_2^2+\omega_2^2)}}, a_1 = \pm\sqrt{\frac{2(\mu_1 k_1^2+\omega_1^2)}{\mu_3}}, a_2 = \pm\sqrt{\frac{2\left(\mu_1 k_2^2+\omega_2^2\right)}{\mu_3}}$,

$\xi_1 = k_1 x - \omega_1 t$, and $\xi_2 = k_2 x - \omega_2 t$.

If we pull-out $b_7 = \frac{2\mu_2}{(\mu_1 k_1^2+\omega_1^2)}, b_8 = 1, b_9 = \frac{2\mu_2}{(\mu_1 k_1^2+\omega_1^2)}, b_{10} = 1$. Then we obtain the hyperbolic function solution

$$u = -\sqrt{-\frac{\mu_2}{\mu_3}}\left(1 + \operatorname{sech}\left(\frac{r\xi_1}{2}\right) e^{\frac{r\xi_1}{2}} + \operatorname{sech}\left(\frac{l\xi_2}{2}\right) e^{\frac{l\xi_2}{2}}\right). \tag{25}$$

If we enclosure $b_7 = -\frac{2\mu_2}{(\mu_1 k_1^2+\omega_1^2)}, b_8 = 1, b_9 = -\frac{2\mu_2}{(\mu_1 k_1^2+\omega_1^2)}, b_{10} = 1$. Then we obtain the hyperbolic function solution

$$u = -\sqrt{-\frac{\mu_2}{\mu_3}}\left(1 + \operatorname{cosech}\left(\frac{r\xi_1}{2}\right) e^{-\frac{r\xi_1}{2}} + \operatorname{cosech}\left(\frac{l\xi_2}{2}\right) e^{-\frac{l\xi_2}{2}}\right). \tag{26}$$

If we insert $b_7 = \frac{2\mu_2}{(\mu_1 k_1^2+\omega_1^2)}, b_8 = 1, b_9 = -\frac{2\mu_2}{(\mu_1 k_1^2+\omega_1^2)},\ b_{10} = 1$. Then we obtain the hyperbolic function solution

$$u = -\sqrt{-\frac{\mu_2}{\mu_3}}\left(1 + \operatorname{sech}\left(\frac{r\xi_1}{2}\right) e^{\frac{r\xi}{2}} + \cos ech\left(\frac{l\xi_2}{2}\right) e^{-\frac{l\xi_2}{2}}\right). \tag{27}$$

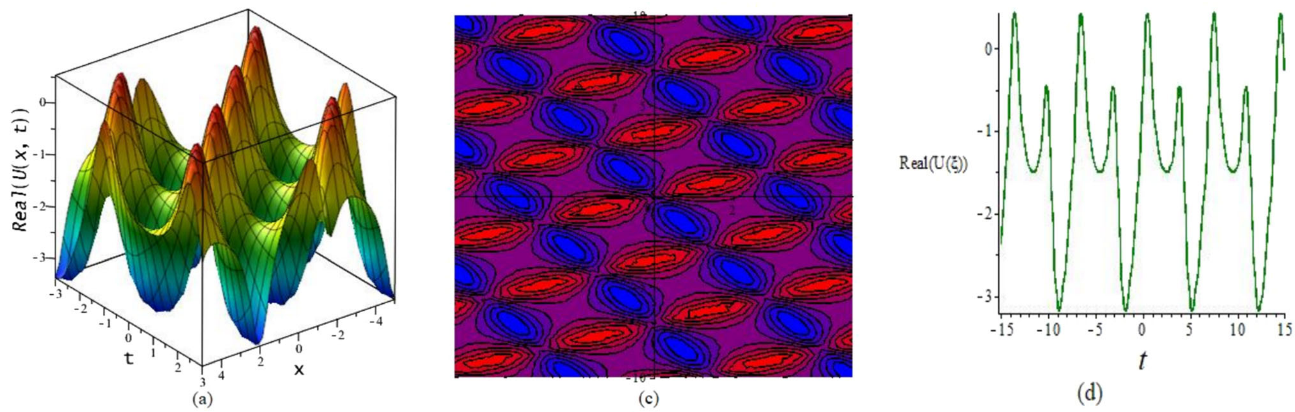

Fig. 6 Feature of the breather wave solution of Eq. (24) for the parameters $k_1 = 0.5,\ k_2 = \omega_1 = 1, \omega_2 = 0.5, \mu_1 = 1, \mu_2 = -2, \mu_3 = -1, l_7 = l_8 = l_9 = l_{10} = 1$. (**a**) is a 3-D plot and (**b**), and (**c**) are corresponding contour and 2-D plots, respectively

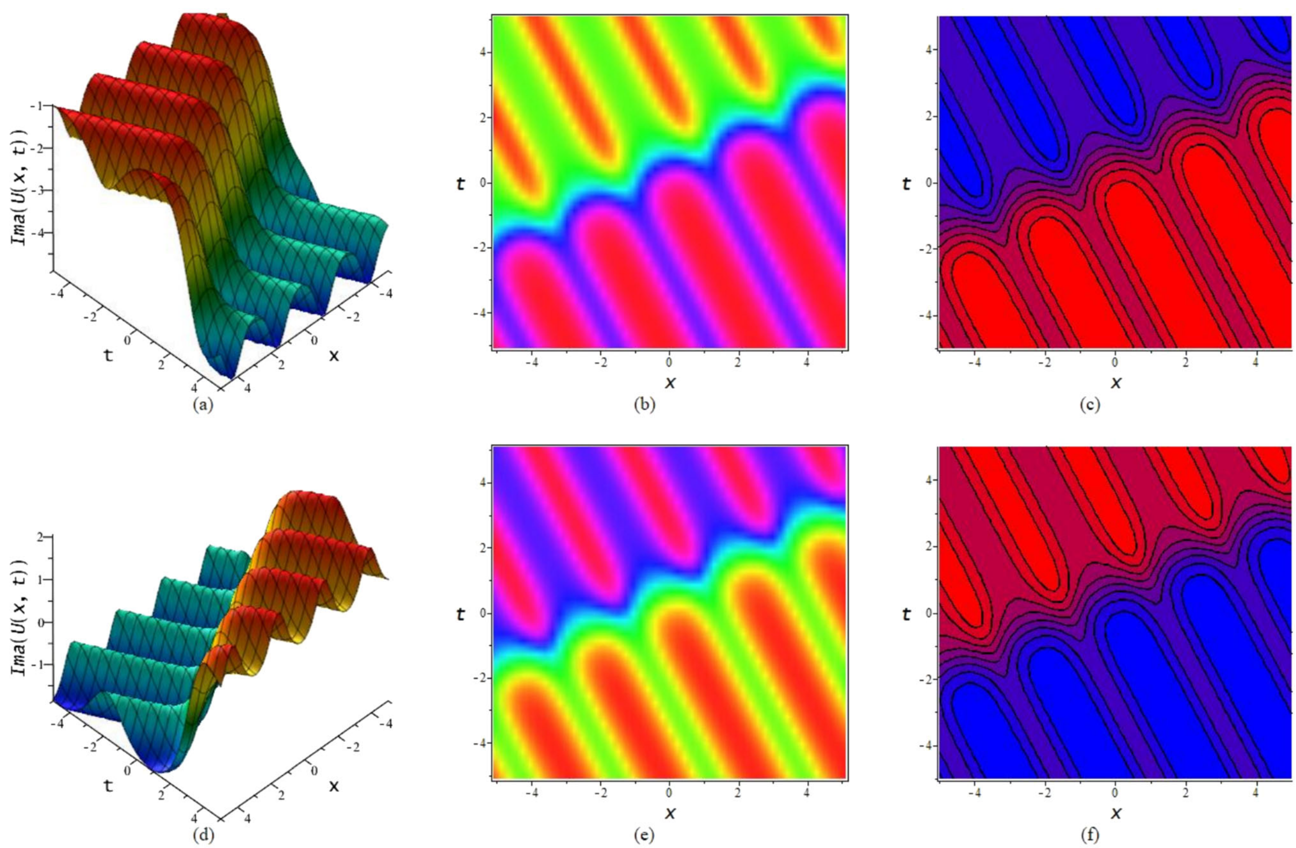

Fig. 7 Feature of the interaction solution of Eq. (24) for the parameters $k_1 = 0.5,\ k_2 = -1, \omega_1 = 1, \omega_2 = 0.5, \mu_1 = -1, \mu_2 = 2, \mu_3 = 1, -l_7 = l_8 = -l_9 = l_{10} = 1$. The figure in (**a**) is a 3-D plot of the interaction of anti-kink and periodic wave solution and (**b**), and (**c**) are corresponding density and contour plots respectively. The figure in (**d**) is a 3-D plot of the interaction of kink and periodic wave solution and (**e**), and (**f**) are corresponding density and contour plots, respectively

4. Numerical results and discussion

In this section, we successfully present the numerical solutions of the obtained solutions graphically with a 3-D diagram with corresponding density and contour diagrams. This section mostly focuses on investigating soliton, multi-soliton, and interaction soliton solutions in this study. Additionally, we present the 3-D diagram, along with the

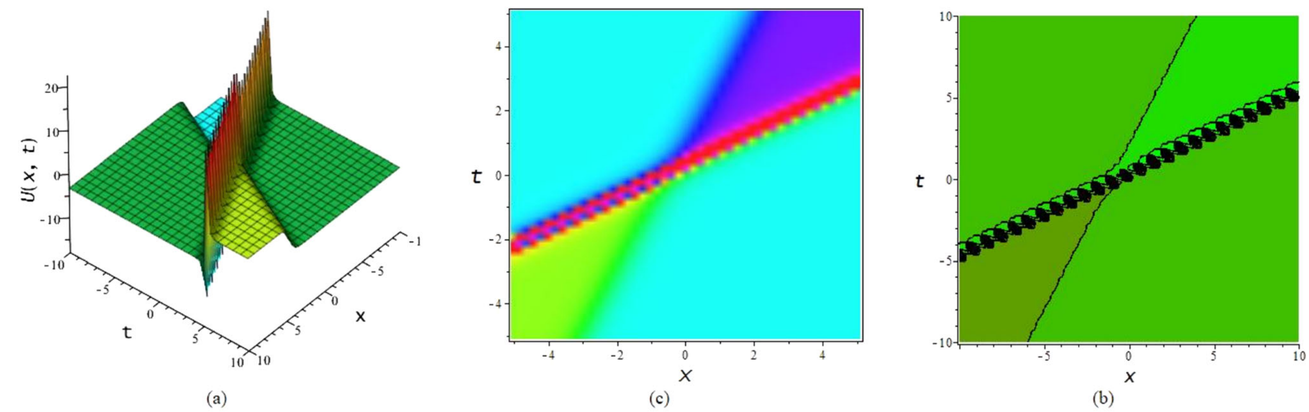

Fig. 8 Feature of the interaction solution between soliton and kink solution of Eq. (24) for the value of the parameters $k_1 = \omega_2 = 0.5,\ k_2 = 1, \omega_1 = 2, \mu_1 = 1, \mu_2 = 10, \mu_3 = -1, -l_7 = l_8 = -l_9 = 2l_{10} = 1$. The figure in (**a**) is the 3-D plot of the interaction solution and (**b**), and (**c**) are corresponding density and contour plots, respectively

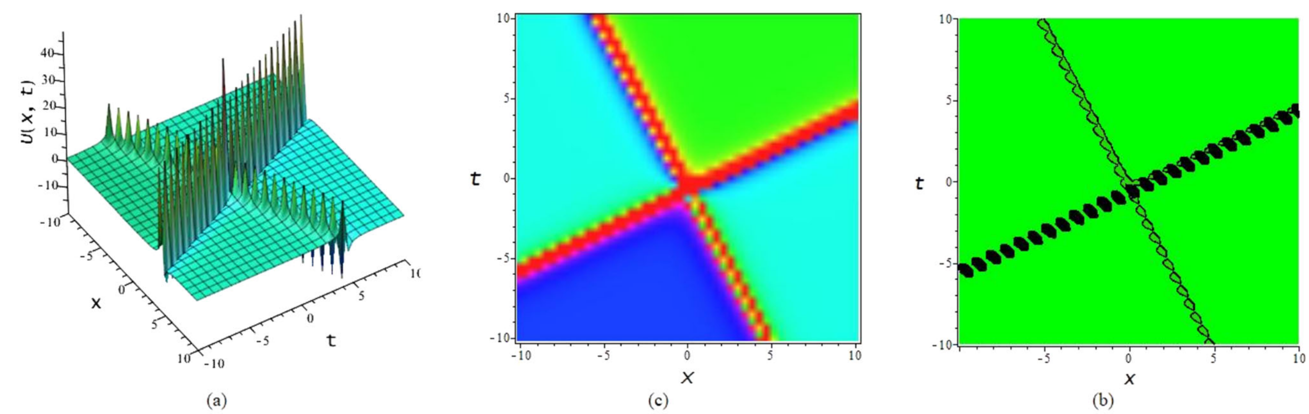

Fig. 9 Feature of the interaction of soliton waves of Eq. (24) for the value of the parameters $k_1 = k_2 = 1, \omega_1 = 2, \omega_2 = -0.5, \mu_1 = 1, \mu_3 = -1, \mu_2 = 1,\ l_7 = l_8 = l_9 = l_{10} = 1$. The figure in (**a**) is the 3-D plot of the interaction solution and (**b**), and (**c**) are corresponding density and contour plots, respectively

corresponding density and contour diagrams, over a specific time frame. We exploit diverse colors to confirm that the wave's conduct will revolutionize, that discrete waves will overlap, or that diverse curves will give the impression at diverse points inside the identical wave.

In this work, all analytical solutions are accessible graphically in Figs. 1, 2, 3, 4, 5, 6, 7, 8, 9, 10, 11, 12, 13 and 14 for special values of the parameters under some conditions. In Fig. 1, we introduce the kink and anti-kink type multi-soliton solution of Eq. (17) at $k_1 = 2,\ k_2 = \omega_1 = 0.5, \omega_2 = 1, \mu_1 = 1, \mu_2 = -2, \mu_3 = -1, l_1 = l_2 = l_3 = l_4 = l_5 = l_6 = 1$. For the condition $a_1 > 0,\ a_2 > 0$, solution of Eq. (17) provides kink type multi-soliton, in (a) is a 3-D plot and (b), and (c) are corresponding density and contour plots respectively. For the condition $a_1 < 0,\ a_2 < 0$, solution of Eq. (17) provides anti-kink type multi-soliton in (d) is a 3-D plot and (e), (f) are corresponding density and contour plots. For the parameters $k_1 = 2,\ k_2 = 0.5, \omega_1 = -1, \omega_2 = -0.5, \mu_1 = 1, \mu_2 = -2, \mu_3 = -1, l_1 = l_2 = l_3 = l_4 = l_5 = l_6 = 1$, we illustrate a novel multi-soliton solution of Eq. (17) in Fig. 2. For the condition $a_1 > 0,\ a_2 > 0$, this solution provides bright multi-soliton in (a) is a 3-D plot and (b), and (c) are corresponding density and contour plots, and for the condition $a_1 < 0,\ a_2 < 0$, the solution provides dark multi-soliton. In Fig. 3, we introduce an innovative interaction solution of Eq. (17) at $k_1 = 2,\ k_2 = \omega_1 = 0.5, \omega_2 = -1, \mu_1 = 1, \mu_2 = -2, \mu_3 = -1, l_1 = l_2 = l_3 = l_4 = l_5 = l_6 = 1$. For the condition $a_1 \langle 0,\ a_2 \rangle 0$, this solution provides interaction with bright and dark bell waves in (a) is a 3-D plot, and (b), and (c) are corresponding density and contour plots, and for the condition $a_1 > 0,\ a_2 < 0$, this solution provides interaction with bright and dark bell waves in (d) is a 3-D plot, and (e), and (f) are corresponding density and contour plots. For the parameters $k_1 = 15,\ k_2 = 1, \omega_1 = 0.01, \omega_2 = 0.5, \mu_1 = 1, \mu_2 = -2, \mu_3 = 1, l_1 = -l_2 = l_3 = l_4 = l_5 = -3l_6 = 1$.

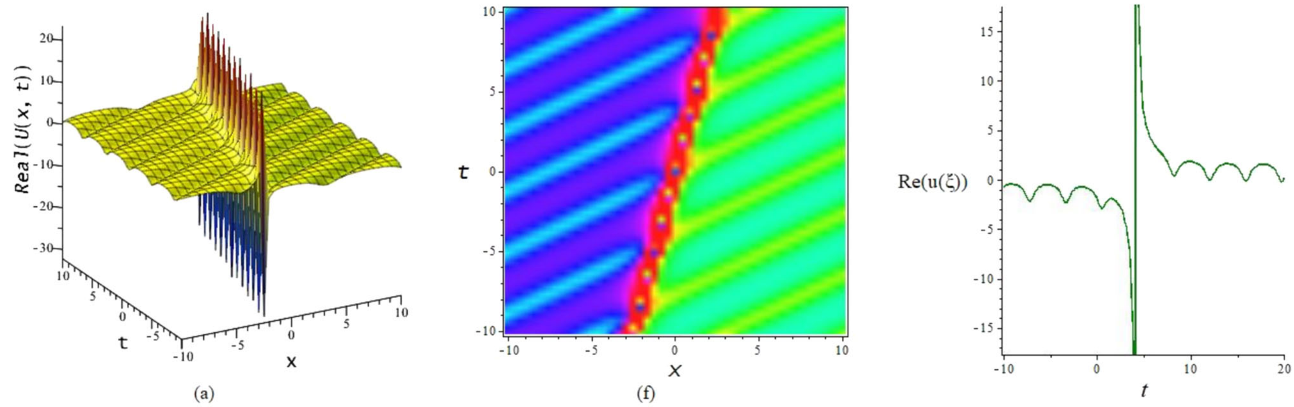

Fig. 10 Feature of the interaction of periodic and singular waves of the solution Eq. (24) for the value of the parameters $k_1 = 0.5, k_2 = 2, \omega_1 = 1, \omega_2 = 0.5, \mu_1 = -1, \mu_2 = -1, \mu_3 = 1,\ l_7 = l_8 = l_9 = 1,\ l_{10} = 2$. The figure in (**a**) is the 3-D plot of the interaction solution and (**b**), and (**c**) are corresponding density and contour plots, respectively

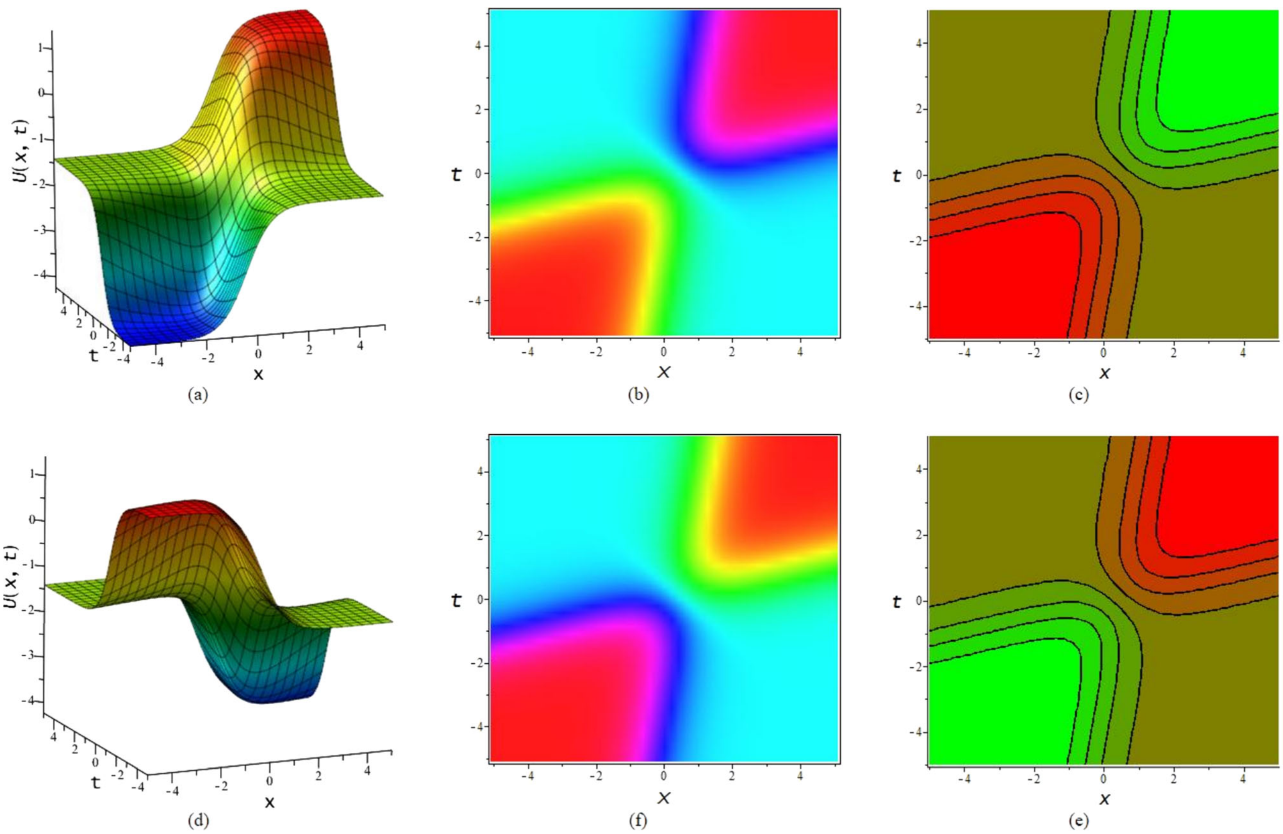

Fig. 11 Feature of the multi-soliton solution of Eq. (26) for the value of the parameters $k_1 = 15,\ k_2 = 1, \omega_1 = 0.5, \omega_2 = -3, \mu_1 = -\mu_3 = 1, \mu_2 = 2$. The figure in (**a**) is a 3-D plot of multi-kink and (**b**), and (**c**) are corresponding density and contour plots respectively. The figure in (**d**) is a 3-D plot of multi-anti-kink (**e**), and (**f**) are corresponding density and contour plots, respectively

We illustrate a novel multi-soliton solution of Eq. (17) shown in Fig. 4. For the condition $\omega_1\langle 0, \omega_2\rangle 0$, this solution provides interaction with dark bell and bright bell wave in (a) as a 3-D plot and (b), and (c) are corresponding density and contour plots, and for the condition $\omega_1\langle 0, \omega_2\rangle 0$, solution of Eq. (17) provides interaction with dark bell and bright bell wave in (d) is a 3-D plot, and (e), and (f) are corresponding density and contour plots. The numerical form of the solution Eq. (17) provides interaction with dark bell and bright bell wave solutions in different forms. For the parameters $k_1 = 15,\ k_2 = 1, \omega_1 = 0.01, \omega_2 = 0.5, \mu_1 = 1, \mu_2 = -2, \mu_3 = 1, l_1 = -l_2 = l_3 = l_4 = l_5 =$

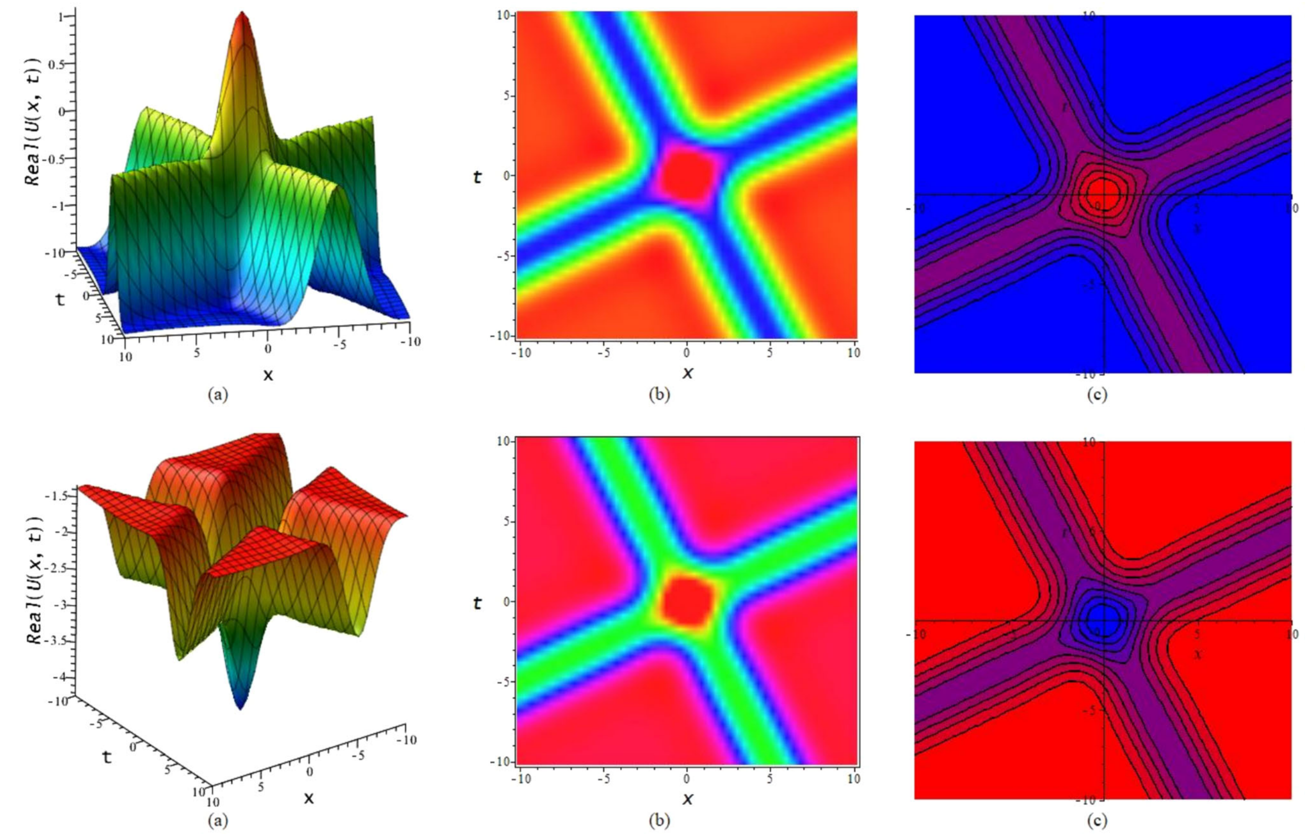

Fig. 12 Feature of the interaction of the double bell wave solution of Eq. (27) for the value of the parameters $k_1 = 0.5,\ k_2 = -1, \omega_1 = 1, \omega_2 = 0.5, \mu_1 = \mu_3 = 1, \mu_2 = -2$. The figure in (**a**) is a 3-D plot of the interaction of bright type double bell wave solution and (**b**), and (**c**) are corresponding density and contour plots respectively. The figure in (**d**) is a 3-D plot of the interaction of dark-type double bell wave solution and (**e**), and (**f**) are corresponding density and contour plots, respectively

$-3l_6 = 1$, we illustrate the graph in Fig. 5. For the condition $\omega_1\langle 0, \omega_2\rangle 0$, this solution provides a breather wave in (a) is a 3-D plot and (b), and (c) are corresponding density and contour plots, and for the condition $\omega_1\langle 0, \omega_2\rangle 0$, this solution provides a breather wave in (d) is a 3-D plot, and (e), and (f) are corresponding density and contour plots.

In Fig. 6, we illustrate the feature of the numerical solution of Eq. (24) for the parameters $k_1 = 0.5,\ k_2 = \omega_1 = 1, \omega_2 = 0.5, \mu_1 = 1, \mu_2 = -2, \mu_3 = \ -1, l_7 = l_8 = l_9 = l_{10} = 1$. The figure in (a) is a 3-D plot and (b), and (c) are corresponding density and contour plots respectively. In Fig. 7, we introduce the interaction solution of Eq. (24) for the parameters $k_1 = 0.5,\ k_2 = -1, \omega_1 = 1, \omega_2 = 0.5, \mu_1 = -1, \mu_2 = \ 2, v_3 = 1, -l_7 = l_8 = -l_9 = l_{10} = 1$. For $a_1 > 0,\ a_2 > 0$, the figure in (a) is a 3-D plot of the anti-kink and periodic solution, and (b), and (c) are corresponding density and contour plots respectively. For $a_1 < 0,\ a_2 < 0$, the figure in (d) is a 3-D plot of kink and periodic solution, and (e), and (f) are corresponding density and contour plots respectively. The interaction solution of the Eq. (24) for the value of the parameters $k_1 = \omega_2 = 0.5,\ k_2 = 1, \omega_1 = \ 2, \mu_1 = 1, \mu_2 = 10, \mu_3 = -1, -l_7 = l_8 = -l_9 = 2l_{10} = 1$ shown in Fig. 8. The figure in (a) is a 3-D plot of the interaction solution between soliton and kink solution and (b), and (c) are corresponding density and contour plots respectively. In Fig. 9, we provide the interaction soliton waves solution of Eq. (24) for the value of the parameters $k_1 = k_2 = 1, \omega_1 = 2, \omega_2 = \ -0.5, \mu_1 = 1, \mu_3 = -1, \mu_2 = 1,\ l_7 = l_8 = l_9 = l_{10} = 1$. The figure in (a) is a 3-D plot of the interaction of solitons and (b), and (c) are corresponding density and contour plots respectively. In Fig. 10, the interaction of the solution Eq. (24) for $k_1 = 0.5, k_2 = 2, \omega_1 = 1, \omega_2 = 0.5, \mu_1 = -1, \mu_2 = -1, \mu_3 = 1,\ l_7 = l_8 = l_9 = 1,\ l_{10} = 2$. The figure in (a) is a 3-D plot of the interaction of periodic and singular waves and (b), and (c) are corresponding density and contour plots respectively. In Fig. 11, the multi-soliton solution illustrates from the Eq. (26) for the value of the parameters $k_1 = 15,\ k_2 = 1, \omega_1 = 0.5, \omega_2 = -3, \mu_1 = -\mu_3 = 1, \mu_2 = 2$. For $a_1 > 0,\ a_2 > 0$, the figure in (a) is a 3-D plot of a multi-kink wave, and (b), and (c) are corresponding density and contour plots respectively. For $a_1 < 0,\ a_2 < 0$ we get the figure in (d) as a 3-D plot of multi-anti-kink wave

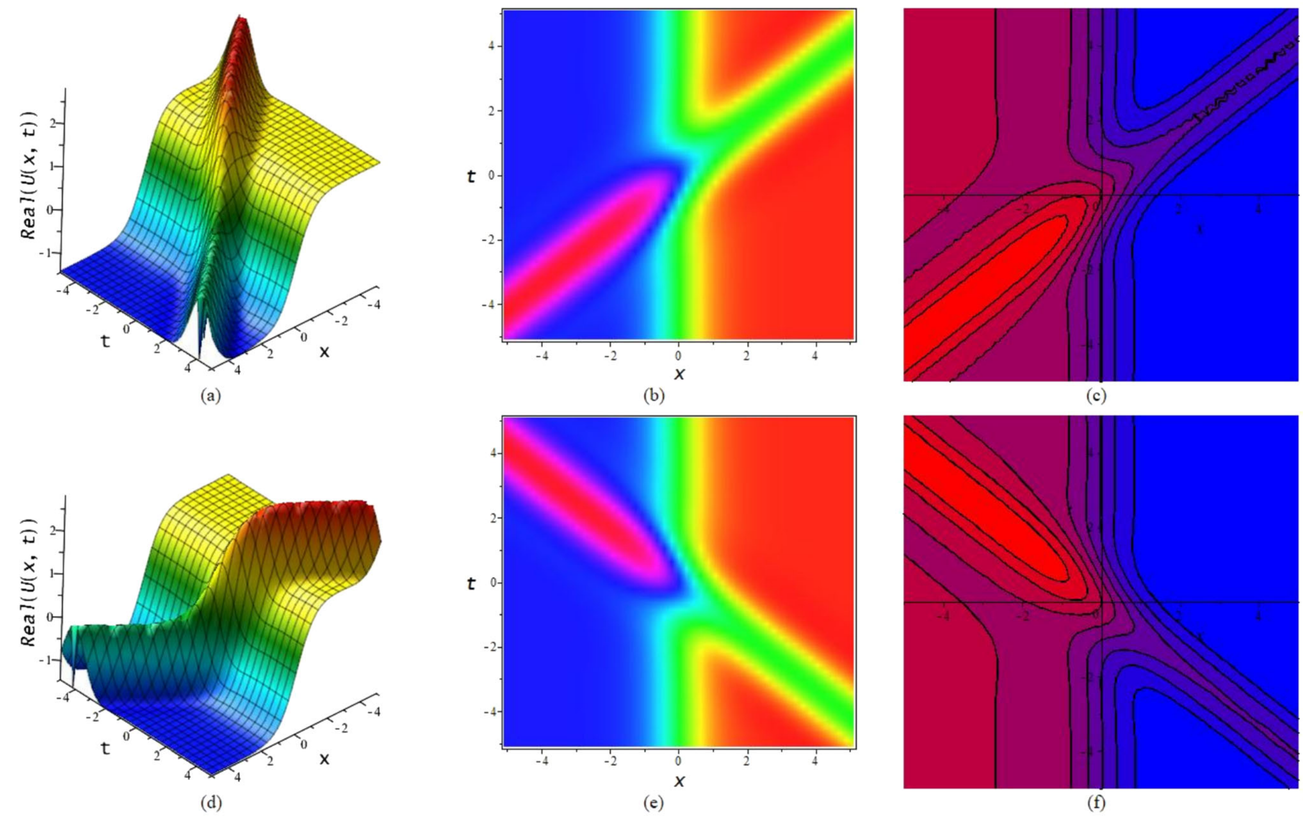

Fig. 13 Feature of the interaction solution of Eq. (27) for the value of the parameters $k_1 = 10, k_2 = -1, \omega_1 = -0.05, \omega_2 = 1.2, \mu_1 = -1, \mu_3 = 1, \mu_2 = -2$. The figure in (**a**) is the 3-D plot of the interaction of the anti-kink and bright bell wave solution, and (**b**), and (**c**) are corresponding density and contour plots respectively. The figure in (**d**) is a 3-D plot of the interaction of anti-kink and bright bell wave solution, and (**e**), and (**f**) are corresponding density and contour plots, respectively

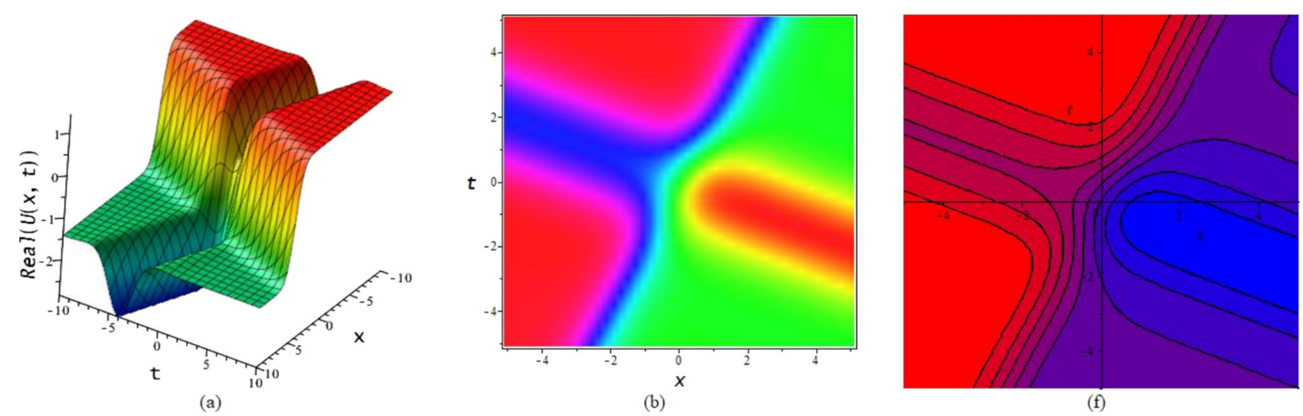

Fig. 14 Feature of the interaction of anti-kink and dark bell wave of Eq. (27) for the value of the parameters $k_1 = 1$, $k_2 = 0.2, \omega_1 = 0.5, \omega_2 = -0.5, \mu_1 = -1, \mu_2 = -2, \mu_3 = 1$. The figure in (**a**) is the 3-D plot of the interaction solution and (**b**), and (**c**) are corresponding density and contour plots, respectively

solution and (e), and (f) are corresponding density and contour plots respectively. Multi-soliton solution of Eq. (27) is demonstrated for the value of the parameters $k_1 = 0.5,\ k_2 = -1, \omega_1 = 1, \omega_2 = 0.5, \mu_1 = \ \mu_3 = 1, \mu_2 = -2$. Shows in Fig. 12. For $a_1 > 0,\ a_2 > 0$, the figure in (a) is a 3-D plot of the bright multi-soliton solution, and (b), and (c) are corresponding density and contour plots respectively. For $a_1 < 0,\ a_2 < 0$, the figure in (d) is a 3-D plot of the dark multi-soliton solution, and (e), and (f) are corresponding density and contour plots respectively. In Fig. 13, the numerical solution of the Eq. (27) for the value of the parameters $k_1 = 10, k_2 = -1, \omega_1 = -0.05, \omega_2 =$

$1.2, \mu_1 = -1, \mu_3 = 1, \mu_2 = -2$. For the condition $\omega_1 = 0.05 > 0, \omega_2 = -1.2 < 0$, the figure in (a) is a 3-D plot of the interaction of anti-kink and bright bell wave solution, and (b), and (c) are corresponding density and contour plots respectively. For the condition $\omega_1 = -0.05\langle 0, \omega_2 = 1.2 \rangle 0$, the figure in (d) is a 3-D plot of the interaction of anti-kink and bright bell wave solution, and (e), and (f) are corresponding density and contour plots respectively. In Fig. 14, the interaction of the anti-kink and dark bell wave solution of Eq. (27) for the value of the parameters $\mathrm{k}_1 = 1,\ \mathrm{k}_2 = 0.2, \omega_1 = 0.5, \omega_2 = -0.5, \mu_1 = -1, \mu_2 = -2, \mu_3 = 1$. The figures in (a) and (d) are 3-D plots of the interaction of anti-kink and dark bell wave solution and (b), (c) and (e), (f)are corresponding density and contour plots respectively.

5. Conclusions

The newly modified simple equation (NMSE) method was successfully applied to the Klein-Fock-Gordon (K-F-G) equation in this study. This allowed the investigation of multi-wave soliton solutions and how they interact with each other. Analytical and graphical techniques were used to derive and visualize these solutions, highlighting the NMSE method's unique capability to address multi-soliton and interaction soliton solutions within this framework—an approach not previously available. Under specific parametric conditions, the solutions were expressed using exponential, trigonometric, and hyperbolic functions, as well as their combinations. For particular parameter values, a variety of soliton configurations were obtained, including multi-kink waves, multi-anti-kink waves, interactions between anti-kink and dark bell waves, anti-kink and bright bell waves, pairs of bright or dark bell waves, bright-dark and dark-bright bell wave interactions, periodic and singular waves, and interactions involving solitons, kinks, anti-kinks, periodic waves, breather waves, and double bright-dark bell wave configurations. These solutions were numerically illustrated through detailed 3D plots, density maps, and contour diagrams, providing a comprehensive perspective on the dynamics of the interactions. This work represents the first analytical derivation and exploration of these solutions, demonstrating their novelty and potential significance. The solutions contribute valuable insights for applications in quantum field theory, particle physics, condensed matter physics, astrophysics, and cosmology. Moreover, the effectiveness and simplicity of the NMSE method in handling multi-soliton and interaction soliton solutions make it a promising tool for nonlinear partial differential equations (NLPDEs). Future studies may focus on exploring modulation instability, chaotic dynamics, and sensitivity analysis incorporating Gaussian and hyperbolic perturbations.

References

[1] B Ghanbari, H Günerhan and S Momani *Phys Scr* **95** 105208 (2020).
[2] A Atangana *Appl Math Comput* **273** 948 (2016).
[3] K U Tariq, A-M Wazwaz and A Ahmed *Opt Quant Electron* **54** 432 (2022).
[4] A M Wazwaz *Comput Math with Appl* **79** 1145 (2020).
[5] S Arshed, A Biswas, P Guggilla and A S Alshomrani *Phys Lett A* **384** 126191 (2020).
[6] S Akter, H-O- Roshid and N F M Noor *Adv Mathematical Phys* **2022** 1 (2020).
[7] M M Roshid, H-O- Roshid, M Z Ali, and H Rezazadeh *Partial Differ Equ Appl Math.* **2** 100012 (2020)
[8] X Yang *Phys Lett A* **449** 128355 (2022).
[9] M Sadaf, S Arshed, G Akram and Iqra *Optik* **268** 169713 (2022).
[10] M M Roshid, T Bairagi, H-O- Roshid and M M Rahman *Partial Differ Equ Appl Math* **5** 100354 (2022).
[11] Z Rahman, A Abdeljabbar, H-O- Roshid and M Z Ali *Fractal Fract* **6** 444 (2022).
[12] H-O- Roshid *Power Res* **6** 49 (2017).
[13] M M Roshid, A Abdeljabbar, A Aldurayhim, M M Rahman, H-O- Roshid, and F S Alshammari *Heliyon.* **8** e11996 (2022).
[14] D Singh, S Yadav and R Arora *Commun Nonlinear Sci Numer Simul* **115** 106786 (2022).
[15] M M Roshid and H Bashar *Math Model Eng Probl* **6** 460 (2019).
[16] H-Y Wu and L-H Jiang *Optik* **262** 169250 (2022).
[17] A Atangana and J Comput *Phys* **293** 104 (2015).
[18] K M Owolabi *Eur Phys J Plus* **135** 864 (2020).
[19] A H Ganie, M M AlBaidani, A-M Wazwaz, W-X Ma, U Shamima and M S Ullah *Opt Quant Electron* **56** 1379 (2024).
[20] M S Ullah, M Z Ali and H-O- Roshid *PLOS ONE* **19** e0307565 (2024).
[21] M S Ullah, M Z Ali and H-O Roshid *Sci Rep* **14** 11907 (2024).
[22] A H Ganie, A-M Wazwaz, A R Seadawy, M S Ullah, H-O-Roshid, H D Afroz, and R Akter Pramana *J Phys.* **98** 46 (2024).
[23] M M Roshid, M Uddin, M M Hossain, and Harun-Or-Roshid *Indian J Phys.* https://doi.org/10.1007/s12648-024-03409-8 (2024)
[24] M M Roshid, M Rahman, M Uddin, and H Or Roshid *Adv Mathematical Phys.* **2024** 6420467 (2024)
[25] M A Akter, G Mostafa, M Uddin, M M Roshid and H O Roshid *Opt Quant Electron* **56** 1255 (2024).
[26] A K Chakrabarty, S Akter, M Uddin, M M Roshid, A Abdeljabbar, and H-O- Roshid *Partial Diff Equ Appl Math.* **11** 100765 (2024).
[27] S Hossain, M M Roshid, M Uddin, A A Ripa and H-O- Roshid *Partial Diff Equ Appl Math* **8** 100551 (2023).
[28] M M Roshid, M Uddin, and G Mostafa *Results Phys.* **51** 106632 (2023)
[29] W-X Ma and T Huang *Phy Scr* **82** 065003 (2010).
[30] W-X Ma, R Zhou and L Gao *Mod Phys Lett A* **24** 1677 (2009).
[31] A Abdeljabbar *Nonlinear Dyn* **110** 3671 (2022).
[32] Z Han and Y Chen *Soc Jpn* **86** 074005 (2017).
[33] Y-L Ma, A-M Wazwaz and B-Q Li *Nonlinear Dyn* **104** 1581 (2021).
[34] Y-L Ma, A-M Wazwaz and B-Q Li *Math Comput Simul* **187** 505 (2021).

[35] P-F Wei, C-X Long, C Zhu, Y-T Zhou, H-Z Yu and B Ren *Chaos Soliton Fract* **158** 112062 (2022).
[36] Gao and L Cheng *Adv Differ Equ.* **2017** 172 (2017)
[37] Y Sun and J Bi *Solitons & Fract* **26** 905 (2005).
[38] A Irshad, S T Mohyud-Din, N Ahmed and U Khan *Results Phys* **7** 4232 (2017).
[39] M N Alam, E Bonyah, M Fayz-Al-Asad, M S Osman and K M Abualnaja *Phys Scr* **96** 055207 (2021).
[40] A R Seadawy, A Ali, H Zahed and D Baleanu *Results Phys* **19** 103565 (2020).
[41] I Ahmad, W A Faridi, M Iqbal, Z Majeed and F Tchier *Int J Theor Phys* **63** 157 (2024).
[42] HU Rehman, I Iqbal, S Subhi Aiadi, N Mlaiki, MS Saleem *Mathematics.* **10** 3377 (2022)
[43] M S Ullah, M Z Ali and H-O- Roshid *Partial Diff Equ Appl Math* **10** 100716 (2024).

Publisher's Note Springer Nature remains neutral with regard to jurisdictional claims in published maps and institutional affiliations.